

# Cutaneous Inputs to Dorsal Column Nuclei in Adult Macaque Monkeys Subjected to Unilateral Lesion of the Primary Motor Cortex or of the Cervical Spinal Cord and Treatments Promoting Axonal Growth

Neuroscience Insights  
Volume 15: 1–13  
© The Author(s) 2020  
Article reuse guidelines:  
sagepub.com/journals-permissions  
DOI: 10.1177/2633105520973991



Julie Savidan<sup>1</sup> , Marie-Laure Beaud and Eric M Rouiller

Faculty of Sciences and Medicine, Fribourg Centre for Cognition, Department of Neurosciences and Movement Sciences, Section of Medicine, University of Fribourg, Fribourg, Switzerland.

**ABSTRACT:** The highly interconnected somatosensory and motor systems are subjected to connectivity changes at close or remote locations following a central nervous system injury. What is the impact of unilateral injury of the primary motor cortex (hand area; MCI) or of the cervical cord (hemisection at C7–C8 level; SCI) on the primary somatosensory (cutaneous) inputs to the dorsal column nuclei (DCN) in adult macaque monkeys? The effects of treatments promoting axonal growth were assessed. In the SCI group ( $n = 4$ ), 1 monkey received a control antibody and 3 monkeys a combination treatment of anti-Nogo-A antibody and brain-derived neurotrophic factor (BDNF). In the MCI group ( $n = 4$ ), 2 monkeys were untreated and 2 were treated with the anti-Nogo-A antibody. Using trans-ganglionic transport of cholera toxin B subunit injected in the first 2 fingers and toes on both sides, the areas of axonal terminal fields in the cuneate and gracile nuclei were bilaterally compared. Unilateral SCI at C7–C8 level, encroaching partially on the dorsal funiculus, resulted in an ipsilesional lower extent of the inputs from the toes in the gracile nuclei, not modified by the combined treatment. SCI at C7–C8 level did not affect the bilateral balance of primary inputs to the cuneate nuclei, neither in absence nor in presence of the combined treatment. MCI targeted to the hand area did not impact on the primary inputs to the cuneate nuclei in 2 untreated monkeys. After MCI, the administration of anti-Nogo-A antibody resulted in a slight bilateral asymmetrical extent of cutaneous inputs to the cuneate nuclei, with a larger extent ipsilesionally. Overall, remote effects following MCI or SCI have not been observed at the DCN level, except possibly after MCI and anti-Nogo-A antibody treatment.

**KEYWORDS:** Spinal cord injury, motor cortex lesion, brain-derived neurotrophic factor, Nogo-A antibody therapy, motor control, transganglionic anterograde tracing

**RECEIVED:** June 17, 2020. **ACCEPTED:** October 27, 2020.

**TYPE:** Original Research

**FUNDING:** The author(s) disclosed receipt of the following financial support for the research, authorship, and/or publication of this article: This work was supported by: Swiss National Science Foundation, Grants No. 31-61857.00, 310000-110005, 31003A-132465, 310030B-149643 (EMR), the National Centre of Competence in Research (NCCR) on “Neural plasticity and repair”, Novartis Foundation; The Christopher Reeves Foundation (Springfield, NJ, USA); The Swiss Primate Competence Centre for Research (SPCCR: [www.unifr.ch/spCCR](http://www.unifr.ch/spCCR)).

**DECLARATION OF CONFLICTING INTERESTS:** The author(s) declared the following potential conflicts of interest with respect to the research, authorship, and/or publication of this article: The anti-Nogo-A antibody was provided by Novartis Pharma AG.

**CORRESPONDING AUTHOR:** Julie Savidan, Faculty of Sciences and Medicine, Fribourg Centre for Cognition, Department of Neurosciences and Movement Sciences, Section of Medicine, University of Fribourg, Chemin du Musée 5, Fribourg CH-1700, Switzerland. Email: [savidan.julie@gmail.com](mailto:savidan.julie@gmail.com)

## Significance Statement

- Primary cutaneous inputs from toes to the gracile nuclei were reduced ipsilaterally after C7–C8 hemisection.
- No effect on the primary cutaneous inputs from fingers to the cuneate nuclei after C7–C8 hemisection or unilateral motor cortex lesions.
- Treatment combining BDNF and anti-Nogo-A antibody did not interfere with the primary cutaneous inputs after C7–C8 hemisection.
- Slightly larger extent of ipsilesional cutaneous inputs to the cuneate nuclei after motor cortex lesion and anti-Nogo-A antibody treatment.

## Introduction

Anatomical reorganizations of the somatosensory pathways resulting from motor system injury remain largely unexplored. Rare studies have reported the possible effects of motor system lesion on the somatosensory system.<sup>1,2</sup> As the first relay of the ascending sensory inputs, the dorsal column nuclei (DCN) might be sensitive to remote effects following injury affecting the motor system at the cortical or at the spinal cord level. Due

to the extent of the cortical and subcortical interconnections, remote effects in other distant areas can be observed following restricted cortical injury,<sup>3</sup> possibly in line with the concept of connectional diaschisis.<sup>4,5</sup> Although the cortico-nuclear projections to DCN originate predominantly from the somatosensory cortex,<sup>6</sup> anatomical and electrophysiological studies have evidenced the existence of projections from the motor cortex and particularly from the primary motor cortex (M1).<sup>6–10</sup> Considering not only the cortical contingent, injury of the motor system at the cortical or at the spinal cord level might result in connectional changes at a distance from the incoming cutaneous inputs to the cuneate nucleus originating from the hand behaviorally affected by the lesion.

Following injury of the central nervous system, 2 main approaches have been proposed to promote axonal regrowth and/or sprouting, either by making the environment permissive to axonal growth or by increasing the level of neurotrophic molecules promoting intrinsic axonal growth. First, based on the characterization of the highly inhibitory properties of the Nogo-A protein in the spinal cord myelin sheath,<sup>11</sup> numerous studies showed the beneficial potentials of blocking this



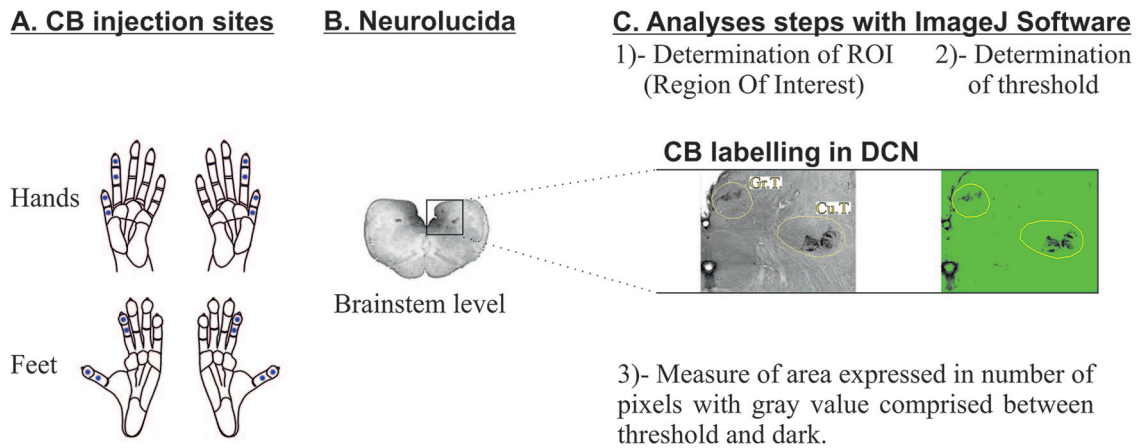


**Figure 1.** Method for analysis of CB. Schematic representations of the Cholera toxin B subunit (CB) transganglionic tracing method, used to visualize the primary somatosensory afferents to the DCN in monkeys subjected to spinal cord injury or to motor cortex injury. For reference, the same tracing protocol was applied to 2 intact monkeys. These schematic representations illustrate: (A) the injection sites (blue dots) of Cholera toxin B subunit (CB) in the 2 distal phalanges of the 2 first fingers/toes of both forelimbs and hindlimbs; (B) Neurolucida images captured with a light microscope of transverse sections of brainstem stained for CB. These sections illustrate the levels of the analyses of primary somatosensory projections to the DCN (CB labeling). (C)

Representation of the dorsal column fasciculi and the consecutive steps for image analyses using imageJ software.

Abbreviations: Cu.N., cuneate nucleus; DCN, dorsal column nuclei; Gr.N., gracile nucleus; T.Cu., tractus cuneatus; T.Gr., tractus gracilis.

molecule and its signaling pathways to promote functional recovery and neural repair in case of spinal cord injury or stroke,<sup>12-18</sup> Treatment with an antibody against Nogo-A promotes functional recovery from spinal cord or motor cortex injuries, enhancing sprouting of corticospinal<sup>19</sup> and lesioned sensory axons<sup>20</sup> promoting reorganization of territories close and distant to the lesion site in rodent,<sup>21-25</sup> in non-human primate<sup>19,26-32</sup> and potentially in human.<sup>33</sup> This anti-Nogo-A antibody treatment has also induced more remote effects, such as the regeneration of lesioned pyramidal projections to the sensory DCN in the brainstem after pyramidotomy in rodent.<sup>22</sup>

Secondly, there has been a large interest in the regeneration promoting role of neurotrophic factors, such as brain derived neurotrophic factor (BDNF),<sup>34</sup> in case of central nervous system injury. BDNF exhibits a promoting role in the survival of axotomized axons, regeneration of injured fibers, plasticity, myelination, and functional recovery.<sup>35,36</sup> It has been highlighted that BDNF can potentiate axonal regrowth alone<sup>37</sup> and also in combination with different molecules.<sup>38</sup> It currently appears that optimal regeneration may well require the application of combined therapies involving several complementary molecules.<sup>39</sup> In the context of SCI, BDNF appeared as a promising therapeutic candidate to be used in combination with the anti-Nogo-A antibody treatment in order to boost functional recovery and axonal regrowth following SCI. Beaud and collaborators<sup>40</sup> have laid out the comprehensive rationale for combining these 2 molecules. The effects of the combined treatment on axonal pathways at the anatomical level remain unknown, especially on the somatosensory pathways. Indeed, in the case of SCI, there is evidence for a re-growth and survival of axotomized ascending somatosensory axons and descending motor axons.<sup>36,41-45</sup> As a consequence, it is pertinent to test the hypothesis that a treatment combining anti-Nogo-A antibody

with BDNF may induce changes in the somatosensory pathway at the brainstem level, remote from the SCI.

The present study aimed at assessing the impacts of 2 different types of lesion, targeting mainly the motor system, on cutaneous inputs from the hand (thumb and index finger) and from the foot (first 2 toes) to the dorsal column nuclei (DCN), namely to the cuneate nucleus and the gracile nucleus, respectively. The first type of lesion is a unilateral spinal (cervical) cord injury (SCI) targeted at C7-C8 level, with the main goal to interrupt the corticospinal tract in the dorsolateral funiculus. However, the injury spread into the dorsal funiculus as well, thus interrupting also some ascending primary sensory inputs. While the median nerve fibers innervating the dermatome including the thumb and the index fingers reach the spinal cord at segments ranging from C5 to T1, a more detailed somatotopic organization can be observed. Darian-Smith<sup>46</sup> have shown in monkeys that the cutaneous inputs from the thumb enter the spinal cord at C6 level and those from the index finger at C7 level. As a result, the cutaneous inputs from the thumb and index finger are most likely spared by a hemi-section located below at C7-C8 level. The second type of lesion is a motor cortex injury (MCI), targeted to the hand area in the primary motor cortex (M1). Moreover, it was our goal to investigate whether a treatment promoting axonal regrowth following injury may intervene in a subsequent step onto these primary cutaneous inputs to the DCN. In a first attempt, the aim was to verify the hypothesis that a C7-C8 spinal cord hemi-section directly impacts the gracile nucleus, reflected by a lower density of the incoming primary sensory axon terminals in the gracile nucleus originating from the ipsilesional first 2 toes (Figure 1). In this context, we aimed to investigate if a treatment combining an antibody against Nogo-A and BDNF<sup>40</sup> may attenuate a bilateral asymmetric CB labeling extent in the gracile nucleus.

Secondly, the aim was to verify that the same C7-C8 spinal cord hemi-section does not affect the primary sensory axons terminating in the cuneate nucleus, originating from the ipsilesional thumb and index finger (Figure 1). Moreover, we aimed to investigate whether the treatment combining an antibody against Nogo-A and BDNF impacts on these unlesioned axon terminals in the cuneate nucleus.

In a third attempt, we investigated the hypothesis whether a unilateral lesion of the hand area in M1 (MCI) might affect at distance the primary sensory (cutaneous) axon terminals in the cuneate nucleus, originating from the ipsilesional thumb and index fingers (Figure 1). As a consequence of the MCI, and in relation to the concept of connectional diaschisis,<sup>5</sup> the terminal field projections of the primary sensory axons in the cuneate nucleus might be affected. This may be triggered by connectional changes of the corticocuneate projections from M1, and/or of the incoming cutaneous inputs to the cuneate nucleus originating from the hand behaviorally affected. A subsequent goal was to investigate whether treatment with the anti-Nogo-A antibody alone following M1 lesion may induce plasticity of the afferent primary projections to the cuneate nucleus.

## Methods

Some methods used in the present study were previously described in detail in previous studies from this laboratory and, therefore, are accessible in the relevant earlier reports cited accordingly below in the corresponding summarized versions. The present analysis represents a side project derived from earlier main studies, specifically designed to investigate the impact of SCI or MCI, as well as the mechanisms of functional recovery in the presence or absence of treatments.<sup>19,27-30,40,47-51</sup>

## Animals

The present study was conducted on 10 adult monkeys (*Macaca fascicularis*; 8 males and 2 females, 3.0 to 5.6 kg; see Table 1), aged 4 to 6 years at the time of the euthanasia. All experiments were carried out in accordance with the Guide for Care and Use of Laboratory Animals (ISBN 0-309-05377-3; 1996) and approved by local veterinary authorities, including the ethical assessment by the local (cantonal) Survey Committee on Animal Experimentation. Final acceptance was delivered by the cantonal and federal Veterinary Offices (Veterinary authorization numbers: FR-175-04, FR-188-06, FR-193-07, FR-157-01, FR-157-03, FR-157-04, and FR-157e-04). The monkeys were obtained either from our colony in our animal facility (before 2010) or were purchased from 2 certified suppliers (BioPrim, 31450 Baziège; France or Harlan Buckshire; Italy).

Monkeys included (Table 1) were originally enrolled in 2 main lesional projects. The monkeys Mk-AB-B, Mk-AB-S, Mk-AB-P, and Mk-C-Bo were subjected to hemi-cervical cord section at C7-C8 level.<sup>19,27,28,40,47-49</sup> The monkeys Mk-A-SL, Mk-A-MO, Mk-C-BI, and Mk-C-RO were subjected to an M1 permanent lesion targeting the hand representation.<sup>29,30,50,51</sup>

These previous studies dealt with motor behavior and reorganization of motor pathways, in the presence or absence of specific treatments. Finally, 2 intact monkeys (Mk-I-R12 and Mk-I-R13) were used as references for comparison with the injured animals.

## Surgery

All surgical procedures were described in detail in previous reports from this laboratory.<sup>19,27,28,30,52-55</sup> To summarize, surgical procedures were conducted under deep anesthesia. Sedation was induced with an injection of ketamine (Ketalar®; Parke-Davis, 5 mg/kg; i.m.) and deep anesthesia was maintained with perfusion of 1% propofol (Fresenius®) mixed with a 5% glucose saline solution (1 volume propofol and 2 volumes of glucose-saline, delivered at a dose of 0.1 mg/kg/min; i.v.). The medication given following sedation induction and during the postoperative period has been detailed in the previous reports from this laboratory cited at the beginning of the surgery section. The surgical facility, under sterile conditions, was approved by the cantonal veterinary office.

## Motor system lesions

**Spinal cord injury (SCI).** Hemilaminectomy procedure to perform a selective hemi-cervical cord lesion was described in detail in previous reports.<sup>19,27,28,40,52,53,55</sup> Briefly, the dorsal root entry zone at the C7 border, covered by the sixth cervical vertebra, was exposed and identified as an anatomical landmark for placing a surgical blade used to perform hemi-section of the cervical cord. The surgical blade was inserted 4 mm in depth orthogonally to the spinal cord and the section was prolonged laterally to completely cut the dorsolateral funiculus. The lesion was located at C7-C8 level, caudal to the main pool of biceps motoneurons but rostral to the pools of triceps, forearm, and hand muscle motoneurons.<sup>56</sup>

**Primary motor cortex injury (MCI) targeting the hand representation.** Cortical lesion required access to M1 with a chronic chamber implant to map the hand representation, allowing targeted lesion of M1 hand area by microinfusion of excitotoxic neurotoxin. Procedures were described in detail in previous reports.<sup>30,50,57</sup> Briefly, under anesthesia, a stainless steel chamber was surgically implanted over the M1 forelimb area, centered at the stereotaxic coordinates 15 mm anterior and 15 mm lateral, and at an angle of 30° with respect to the mid-sagittal plane, allowing perpendicular electrode penetrations with respect to the cortical surface, in order to map M1 with intracortical microstimulation (ICMS) in the awake monkey.<sup>30,57,58</sup> Lesion of M1 was induced by ibotenic acid (Sigma; 10 µg/µl in phosphate buffer) infusion at cortical ICMS sites eliciting fingers movements at low intensity of stimulation. Using a Hamilton microsyringe, a volume of 1 µl to 1.5 µl of the ibotenic acid solution was injected at each site (for more detail see Liu and Rouiller and Savidan et al<sup>57,58</sup>). The total volume and numbers of ICMS sites infused with ibotenic acid are listed in Table 1.

Table 1. Summary of animals.

	INTACT MONKEYS			SPINAL CORD INJURED MONKEYS (SCI)				MOTOR CORTICAL INJURED MONKEYS (MCI)			
	Mk-I-R12	Mk-I-R13		Mk-C-BO	Mk-AB-B	Mk-AB-S	Mk-AB-P	Mk-C-RO	Mk-C-BI	Mk-A-MO	Mk-A-SL
General	Female	Female		Male	Male	Male	Male	Male	Male	Male	Male
Sex	Own colony	Own colony		Bio Prim	Bio Prim	Buckshire US	Buckshire US	Bio Prim	Bio Prim	Bio Prim	Bio Prim
Origin of monkeys	4	3	3.5	5.3	4.2	4.6	3.2	5	5.6	4.6	4.6
Weight	6	4.5	4.5	6.5	4.5	5	5	6	6	6.5	6.5
Age at the sacrifice (rounded 0.5 year)	Spinal			Right	Left	Left	Left	Left	Left	Left	Left
Hemi-spinal lesion side				J+192	J+167	J+173	J+180				
Survival time with respect to lesion day (J0)				93	83	93	77				
Hemisection extent (%)				4.11	2.36	10.37	6.2				
Volume of lesion (mm <sup>3</sup> )								Left	Left	Left	Left
Hemisphere lesion side								J+286	J+301	J+195	J+271
Survival time with respect to lesion day (J0)								18 (in 12 cortical fingers ICMS sites)	29.7 (in 29 cortical fingers ICMS sites)	20 (in 20 cortical fingers ICMS sites)	18 (in 12 cortical fingers ICMS sites)
Volume of ibotenic acid injected (μL) (Number of ICMS sites of injections)								0	0	0	1.8
Volume of lesion in post-central gyrus (mm <sup>2</sup> )											
Total volume of lesion (in mm <sup>3</sup> ) Gray matter (motor cortex + post-central gyrus)								14	20.13	41.8	78.2
Treatment				Control antibody	BDNF & hNogo-A	BDNF & hNogo-A	BDNF & hNogo-A	Untreated	Untreated	11C7	11C7
Concentration				7 mg/ml	18mg/ml 0.7mg/ml	18mg/ml 0.7mg/ml	18mg/ml 0.7mg/ml			3mg/ml	3mg/ml
Volume of pumps (ml) for delivery				2	2	2	2			2	2
CB volume (μl) and concentration (%)	160; 0.5%	160; 0.5%	160; 0.5%	160; 0.5%	170; 0.5%	160; 0.5%	160; 0.5%	160; 0.5%	160; 0.5%	160; 0.5%	120; 0.5%
Volumes per injections sites (μl)	10per Hands & feet D1 & D2 DP & MP	10per Hands & feet D1 & D2 DP & MP	10per Hands & feet D1 & D2 DP & MP	10per Hands & feet D1 & D2 DP & MP	15 in Hands-D1-DP + 10per Hands-D2-DP Hands-D1 & D2-MP Feet-D1 & D2-DP & MP	10per Hands & feet D1 & D2 DP & MP	10per Hands & feet D1 & D2 DP & MP	10per Hands & feet D1 & D2 DP & MP	10per Hands & feet D1 & D2 DP & MP	7.5per Hands & feet D1 & D2 DP & MP	7.5per Hands & feet D1 & D2 DP & MP
CB transport time (days)	14	14	8	7	12	12	12	7	12	6	14

Individual data for each monkey included in the present study. Mk-AB- corresponds to the control antibody treated group, Mk-AB- to the combined treated group (anti-Nogo-A and BDNF treatment), Mk-A- to the anti-Nogo-A antibody treated group and Mk-I- to the intact group. (J+) corresponds to the number of days from the lesion day (J<sub>0</sub>). Sites of Cholera toxin subunit B (CB) injections: D1 for thumb and D2 for index; DP for distal phalange and MP for medial phalange.



## Treatment

Concerning monkeys subjected to spinal cord injury (SCI), as previously reported (for anti-Nogo-A antibody treatment<sup>19,27,28,40,47,53</sup>; for combined treatment with anti-Nogo-A antibody and BDNF<sup>40,48</sup>), the tested treatment was administered at the day of the lesion with osmotic minipumps connected to a catheter inserted intrathecally in the vicinity of the cervical lesion site. As indicated in Table 1, 1 SCI animal received a control antibody (Mk-C-Bo), a purified IgG of a mouse mAb (monoclonal antibody) directed against wheat auxin (AMS Biotechnology, Oxon, United Kingdom; 14.8 mg over 4 weeks). Three SCI animals (Mk-AB-B, Mk-AB-S, and Mk-AB-P) were treated via 2 minipumps: a first one delivering a monoclonal anti-Nogo-A antibody (14.8 mg in 4 weeks), and a second one delivering the neurotrophic factor BDNF (1.4 mg in 4 weeks). The minipumps were removed after 4 weeks. The rationale for combining these 2 treatments were reported in detail in a recent report.<sup>40</sup> Concerning monkeys subjected to motor cortex injury (MCI), as previously reported,<sup>29,30,51</sup> the tested anti-Nogo-A antibody (11C7, 3 mg/ml) treatment was administered at the time of the lesion via 2 osmotic minipumps implanted in the neck region (Alzet®, model 2ML2, 5 µl/h) in 2 MCI animals (Mk-A-SL and Mk-A-MO). The first pump was connected to a catheter inserted intrathecally at C7-C8 cervical spinal cord level (as described above for spinal cord injury minipump implant). The second pump was connected to a catheter tunneled under the skin up to the head and the tip pushed under the dura through a small opening in the skull in close proximity to the motor cortex to infuse the lesion territory vicinity. The minipumps were removed after 4 weeks. The 2 animals in the control group did not receive any treatment (Mk-C-BI and MK-C-RO, untreated) and thus were not implanted with minipumps.

Two monoclonal antibodies were used in this study, characterized in detail by Freund et al,<sup>28</sup> both identifying in a mono-specific manner the primate-Nogo-A protein<sup>40,59,60</sup>: the mAb hNogo-A and the 11C7 (Table 1).

## Tracer injections

The transganglionic method of tracing of the primary somatosensory afferents to the dorsal column nuclei (DCN) is similar to that used by Darian-Smith,<sup>61</sup> except that it was not restricted to hand (thumb and index finger) but extended here to the foot (first 2 toes) and that we used unconjugated Cholera toxin B subunit (CB: 0.5% in distilled water, Sigma-C9903). This method of transganglionic tracing following subcutaneous injections in the forelimb and hindlimb has been reported in earlier reports as well.<sup>62-67</sup> Briefly, CB has been used as transganglionic tracer to selectively label ascending primary somatosensory axons and their terminal fields in the DCN in the brainstem (Figure 1). CB was injected sub-dermally under anesthesia (a mixture of ketamine and medetomidine, s.c.),

with a Hamilton microsyringe, in the 2 distal phalanges of the first (thumb/first toe) and second (index/second toe) fingers of the 4 limbs (Figure 1A). For each injected finger or toe, there was 1 syringe penetration in each of the 2 distal phalanges (DP: distal phalange and MP: medial phalange) and, along with each syringe penetration, the volume of tracer injected was delivered at 3 injection sites per phalange. The sites and the volumes of injections are detailed in Table 1. A survival period of at least 1 week (more detail in Table 1) was observed to allow CB transport to the brainstem.

## Histology

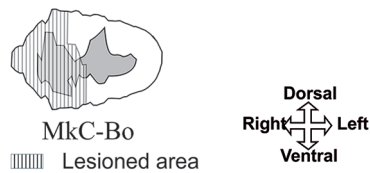
**Anatomical reconstruction.** At the end of the experiments, monkeys were deeply anaesthetized with ketamine and received a lethal dose of sodium pentobarbital (90 mg/kg; i.p.) before a transcardiac perfusion with paraformaldehyde (4%) in 0.1 M of phosphate buffer (pH=7.6) in order to fixate tissue, followed by solutions of increasing concentration of sucrose<sup>40,47,55</sup> (10%, 20%, and 30%). Brain, brainstem, and spinal cord were extracted and immersed into a sucrose solution (30% in phosphate buffer, pH=7.6). For the anatomical reconstruction of spinal cord lesion (Figure 2), the spinal cord block of the lesion site (C6-T3) was sectioned in 3 series of 50 µm thick (0.15 mm interval) parasagittal sections. One of the 3 series was stained with SMI-32 for anatomical reconstruction of the lesion. Method for SMI-32 staining was already described in previous reports<sup>47,48</sup> as well as the anatomical reconstruction of the lesion.<sup>19,40,47,52,55</sup> Drawings of the borders of the lesion sites and contours of the different part of the spinal cord were aligned to allow the reconstruction showing the location and the extent of the lesion in the spinal cord on a transverse view and to calculate the volume of the lesion in mm<sup>3</sup>.

For the anatomical reconstruction of the motor cortical lesion (Figure 2), the brain was sectioned into 50 µm thick coronal sections. Out of 5 series of sections, 1 series was stained for anatomical reconstruction of the lesion with the SMI-32 marker. Under a light microscope and using Neurolucida software, consecutive sections labeled for SMI-32 marker (0.25 mm interval) were used to draw borders and contours of the lesion site in M1, delimited based on cortical layer V interruptions.<sup>30</sup> The lesion site corresponds to the cumulated volume in mm<sup>3</sup> of regions where the cortical layer V was deprived of SMI-32 positive pyramidal neurons (Table 1), calculated by extrapolation with a specific tool of the Neurolucida software using the Cavalieri method.<sup>68</sup>

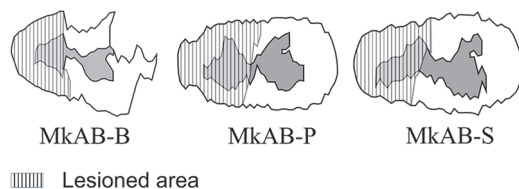
**CB immunohistochemical staining.** The brainstem was sectioned in 3 (Mk-A-Sl, Mk-C-Ro, Mk-A-Mo) or 5 (Mk-I-R12, Mk-I-R13, Mk-ABB, Mk-AB-S, Mk-AB-P, Mk-CBo, Mk-C-Bi) series of 50 µm thick (respectively 0.15 mm or 0.25 mm interval) transversal sections and 1 series was used for CB immunohistochemical staining. The method described by

### A. SCI: transverse cervical cord view

#### Control antibody treated



#### Anti-Nogo-A antibody & BDNF treated



### B. MCI: left hemisphere view

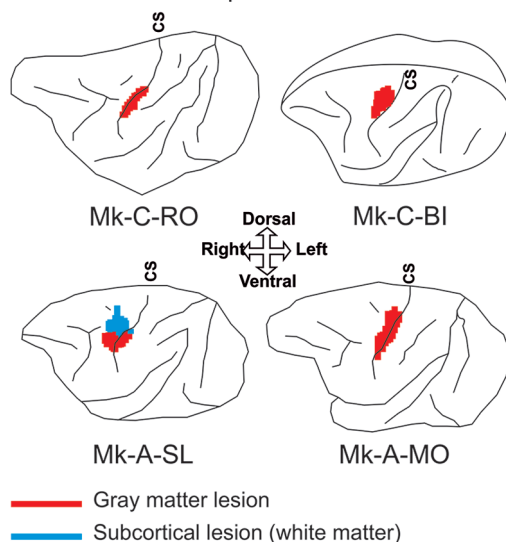


**Figure 2.** Representation of the spinal cord and motor cortical injury. For each monkey injected with CB, reconstruction of the spinal cord injury (SCI) on a transverse section at C7-C8 level (panel A) and the unilateral motor cortex injury (MCI) on a schematic lateral view of the brain (panel B). CS, central sulcus. Panel A. Monkeys subjected to SCI and to the administration of either a control-antibody or a combined anti-Nogo-A antibody associated with BDNF treatment. The striped areas over the transverse sections of the spinal cord represent the lesioned area. Panel B. Monkeys subjected to MCI and either not receiving treatment or receiving the anti-Nogo-A antibody treatment. Color code differentiates cortical injury in the gray matter injury (red) and subcortical injury in the white matter (blue). Same reconstructions as shown in previous reports (SCI<sup>19,27,28,40,47-49</sup> and MCI<sup>29,30,50,51</sup>). The lesion representation crossing the central sulcus symbolized the perpendicular lesioned territory located in the rostral wall of the central sulcus in the hand area of the primary motor cortex (M1).

Rouiller et al<sup>69</sup> was used to reveal the transganglionic tracer CB. Briefly, the sections were rinsed in a solution of Tris buffered saline (TBS-T, 0.05M, pH 8.6) with Triton X100 at 0.5% before overnight incubation at 4°C with primary antibody against CB (Goat anti-choleraenoid; List Biological

Laboratories-Product numero: 703; 1:10 000). Sections were rinsed with TBS-T and incubated with a secondary antibody Rb-anti-goat IgG (Sigma, 1:40) diluted in TBS-T for 90 minutes at room temperature. An amplification step was performed with the peroxidase anti-peroxidase (PAP) method by incubation with goat PAP (Nordic, 1:400) diluted in TBS-T for 90 minutes. Immunohistostaining was revealed with a 0.05% Diaminobenzidine (DAB) solution in Tris-HCL (0.05M, pH 7.6) buffer in 2 steps: a first preincubation step of 15 to 30 minutes and the second step of 30 minutes incubation with the addition of 0.01% H<sub>2</sub>O<sub>2</sub>.

### Histological analysis

Images were captured using Neurolucida software (MicroBrightField, Williston, VT, USA) from light microscope (Olympus) at 12.5× magnification (Figure 1B). For each monkey, images of all sections were captured at once and under the same light conditions. Images were analyzed using NIH ImageJ software (Dr Wayne Rasband, National Institutes of Health, Bethesda, MD) (Figure 1C). The CB staining was analyzed in grayscale intensity by processing images in 8 bits gray type. Regions of interest (ROI) were drawn, surrounding the bilaterally observed CB staining territory in the DCN. Both the cuneate and gracile nuclei were analyzed in monkeys subjected to SCI, as well as in intact monkeys. Only the cuneate nucleus was analyzed in monkeys subjected to MCI given that the injury was restrained to the hand motor area. Staining was measured by the number of pixels in the delimited ROIs. A threshold was determined for each monkey to select pixels with gray value corresponding to the CB staining. As for pictures acquisition under the microscope, all parameters were kept constant for the staining measurement all along the brainstem sections in the same subject. The extent of the CB labeling is illustrated with bar graphs representing the whole labeling observed in each DCN from the first slide presenting CB labeling to the last slide presenting CB labeling along the caudo-rostral axis, each bar representing the area of labeling per slide (Figures 3-5B, C and D). For each monkey, CB staining was compared between the 2 sides of each section as paired values with the non-parametric Wilcoxon test.

### Results

The different groups of monkeys are listed in Table 1, consisting in 2 intact monkeys (Mk-I-R12 and Mk-I-R13) as references, 4 monkeys subjected to spinal cord injury (SCI: hemi-section at cervical level) and 4 monkeys subjected to motor cortex injury (MCI: unilateral lesion in M1 hand area). In the SCI group, 1 monkey received a control antibody treatment whereas in the other 3 monkeys a mixed anti-Nogo-A/BDNF treatment was administered. In the MCI group, 2 monkeys of the control group were untreated whereas the other 2 received an anti-Nogo-A antibody treatment. The extent and location of the lesions are shown in Figure 2.

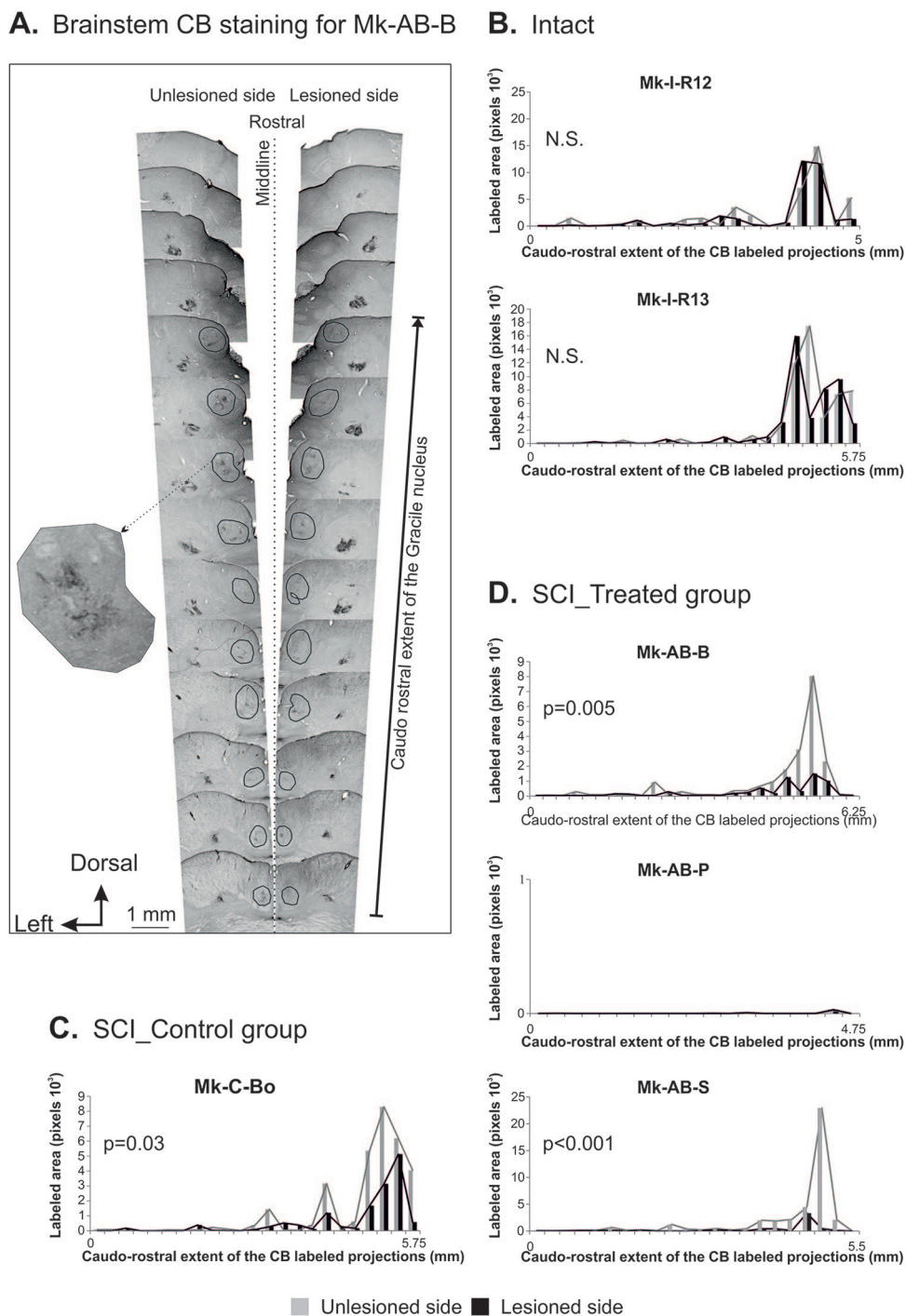


**Figure 3.** SCI-Gracile nucleus: CB labeling. Panel A. Distribution of the CB labeled primary somatosensory axonal terminal fields bilaterally in the gracile nucleus (within the black circles), as seen on histological sections arranged from rostral (top) to caudal (bottom) in Mk-AB-B. Note the presence of CB labeling in the cuneate nucleus as well, more laterally on both sides. Panels B, C, D. The bar graphs represent the extent of the CB labeled axonal terminal fields given by the number of pixels measured with imageJ software on each individual brainstem section, along the caudo-rostral axis, and on each side of the brainstem. These data are shown separately for 2 intact monkeys (panel B), the monkey treated with the control antibody (panel C), and the monkeys treated with the mixture of anti-Nogo-A antibody + BDNF (panel D). In panels C and D, the data for the ipsilesional gracile nucleus are depicted in black and for the contralesional gracile nucleus in gray. A distance of 250  $\mu$ m separates 2 consecutive sections along the caudo-rostral axis in all monkeys. Comparison of the lesioned side versus the unlesioned side with the non-parametric Wilcoxon test for paired values: N.S. is for a statistically non-significant difference.

### CB labeling in DCN

Primary somatosensory axon terminal projections originating from the 2 distal phalanges of the first and second digits of the

4 limbs were assessed in the DCN by measuring CB labeling areas in DCN along the caudorostral axis (Figure 1B). The areas of CB labeled axonal terminal fields in the gracile nucleus



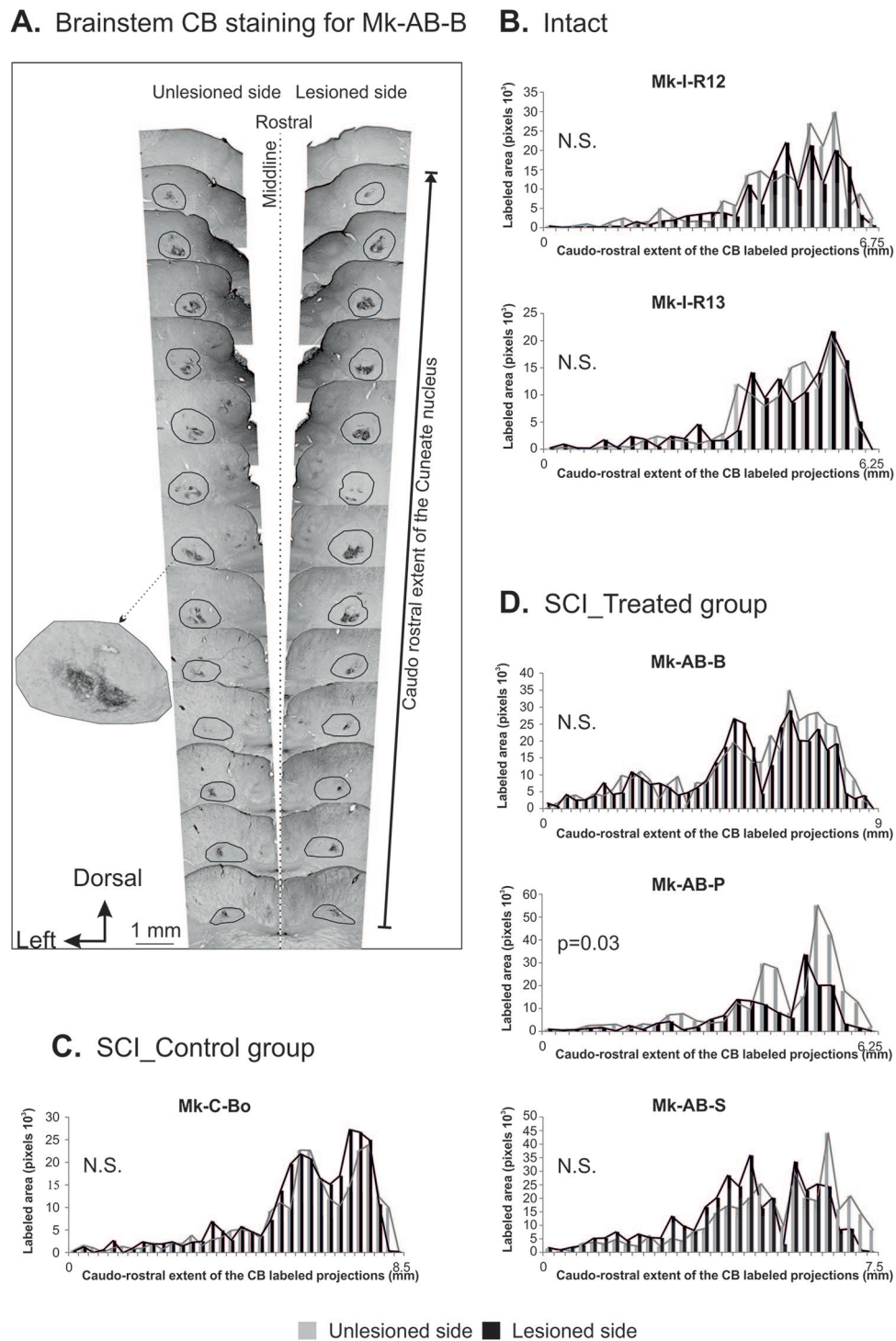


**Figure 4.** SCI-Cuneate nucleus: CB labeling. Same data as in Figure 3, but for CB labeling in the cuneate nucleus (within the black circles), for the same monkey groups, as described in the legend of Figure 3.

(Figure 3) and the cuneate nucleus (Figures 4 and 5) were compared between the 2 sides of the brainstem in the different groups of monkeys.

*Gracile nucleus, effects of SCI.* The CB-labeled terminal fields in the gracile nuclei are illustrated for Mk-AB-B in Figure 3A on individual sections along the caudo-rostral axis. The area of CB-labeled terminal fields on each side was plotted as

a function of the caudo-rostral axis in Figures 3B, C, and D in the 3 groups of monkeys. In intact monkeys, the CB-labeling was most extensive in the rostral pole of the gracile nuclei, without a statistically significant bilateral difference (N.S.; Figure 3B). In the monkeys subjected to SCI (Figure 3C and D), the CB labeling was also most extensive in the rostral pole of the gracile nuclei, though less prominently than in the intact monkeys. However, as expected, the SCI monkeys



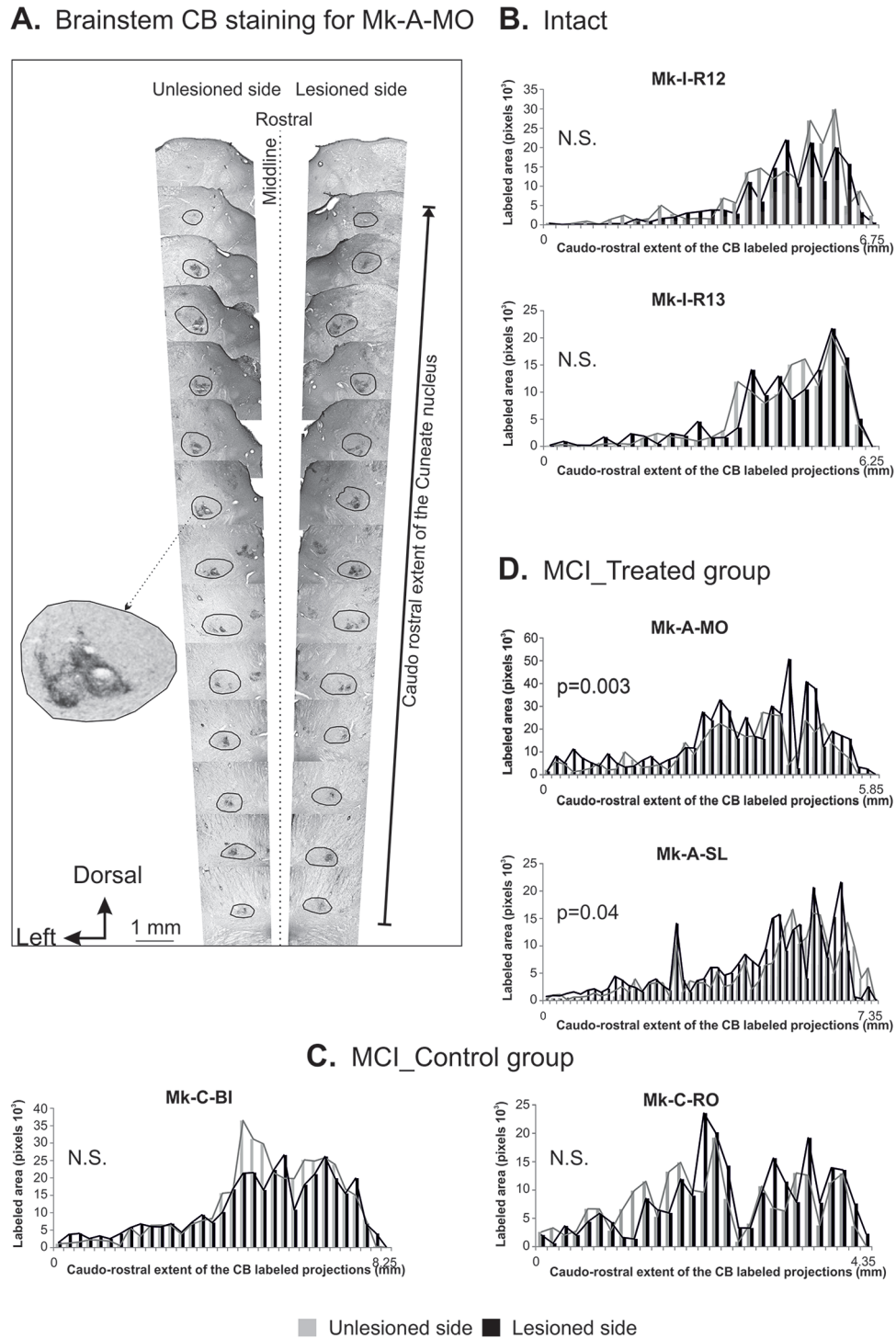


**Figure 5.** MCI-Cuneate nucleus: CB labeling. Same data as in figure in Figure 4 (CB labeling in the cuneate nucleus), but for other groups of monkeys, subjected to MCI. The CB labeling area data of reference in intact monkeys (panel B) are the same as in panel B of Figure 4. In panel C, data for 2 untreated MCI monkeys whereas panel D illustrates 2 MCI monkeys treated with the anti-Nogo-A antibody. A distance of 250  $\mu$ m separates each section along the caudo-rostral axis for intact monkeys and Mk-C-BI, but of 150  $\mu$ m for the other monkeys subjected to MCI: Mk-A-SL, Mk-A-MO, and Mk-C-RO. Conventions as in Figures 3 and 4.

exhibited a bilateral imbalance of CB-labeling area, diminished on the ipsilesional side as compared to the contralesional (not affected) side. This bilateral area difference was statistically significant in 3 SCI monkeys (Figure 3C and D), whereas there was no CB labeling in the gracile nuclei in the

fourth monkey (Mk-AB-P), possibly due to a failure of the injections in the hindlimb (but not forelimb, see below). Note that the largest bilateral imbalance was found in the monkey (Mk-AB-S) subjected to the largest cervical cord lesion (see Table 1: 10.4 mm<sup>3</sup>).

*Cuneate nucleus, effects of SCI.* Typical labeling in the cuneate nuclei resulting from CB injection in the hand (2 distal phalanges of thumb and index finger bilaterally) is illustrated in Figure 4A for monkey MK-AB-B. As observed for the gracile nuclei, the extent of CB labeling in the cuneate nuclei was most prominent rostrally, without bilateral difference in the 2 intact monkeys (Figure 4B). In the SCI monkeys, the same caudorostral bias was observed (Figure 4C and D). Besides, there was no bilateral difference in CB labeling in 3 out of the 4 SCI monkeys (N.S.). The exception was monkey Mk-AB-P with a larger statistically significant CB-labeled terminal field on the unlesioned side ( $P=.03$ ).

*Cuneate nucleus, effects of MCI.* Typical CB-labeling in the cuneate nucleus in a monkey subjected to MCI is illustrated in Figure 5A on individual sections along the caudorostral axis. As the same 2 intact monkeys (Figure 5B), the 2 MCI monkeys of the control group also showed no significant bilateral difference (Figure 5C: N.S.) and a CB labeling most extensive rostrally, though somewhat less than the intact monkeys. In contrast, the 2 MCI monkeys which received the anti-Nogo-A antibody treatment exhibited a bilateral asymmetric CB labeling extent in the cuneate nuclei, with a significantly larger extent in the ipsilesional cuneate nucleus (Figure 5D;  $P=.04$  and  $P=.003$ ). Besides the treatment, the 2 monkeys Mk-A-SL and Mk-A-MO were subjected to a larger M1 lesion than the 2 MCI monkeys of the control group (Table 1).

## Discussion

### *Summary and limitations of the present CB tracing data*

The main results of this study can be summarized as follows: (1) Hemi-cervical cord lesion at C7-C8 level gave rise to a direct massive deficit of primary somatosensory (cutaneous) projections to the gracile nucleus originating from the first 2 ipsilesional toes. This deficit was not attenuated by the combined BDNF and anti-Nogo-A antibody treatment; (2) Hemi-cervical cord lesion at C7-C8 level, or lesion in M1 hand area, in general, did not impact on the bilateral balance of the primary somatosensory projections to the cuneate nucleus, originating from the first 2 hand fingers. The exception was observed for 1 SCI monkey treated with the combined antibody, the area of cutaneous terminal projection in the cuneate nucleus being slightly smaller on the lesioned side, (Mk-AB-P, Figure 4D) and the 2 MCI monkeys treated with the anti-Nogo-A antibody (Figure 5D), the area of cutaneous terminal projection in the cuneate nucleus being slightly larger on the lesioned side.

Before discussing the results, it has to be kept in mind that the conclusions are mainly limited by the fairly restricted number of cases, although this is often the case for non-human primate investigations. In particular, in the SCI group, the monkeys injected with CB in the hand and foot reported in the

present study were among the last ones in the overall project (mostly those treated with the combined treatment anti-Nogo-A antibody with BDNF),<sup>40</sup> whereas CB was not injected in early SCI monkeys (mostly those performed earlier and treated with a control antibody or anti-Nogo-A antibody alone).<sup>19,27,28</sup> Thus, a study including additional CB injected monkeys subjected to control antibody treatment (only 1 reported here) or to anti-Nogo-A antibody treatment (none available) would give a more comprehensive investigation of the various treatments' effects on cutaneous inputs to the DCN after SCI.

The 2 types of unilateral lesion reported in the present study (SCI or MCI) are quite different, although they both lead to a disturbance of the manual dexterity of the related hand. However, MCI (limited to the hand area of M1) led to a pure deficit of manual dexterity whereas SCI (nearly cervical hemisection) produced a deficit of the ipsilesional hand accompanied by hindlimb dysfunction as well. There was no intention here to compare the 2 types of lesion, which should be considered separately. Indeed, the goal of the SCI was to assess direct effects of the lesion on an impacted pathway, namely the cutaneous inputs from the hindlimb, testing the possible impact of the combined treatment. In the MCI lesion model, the aim was to test whether the cortical lesion may induce a distal connective change at distance on cutaneous inputs to the cuneate nucleus, originating from the behaviorally affected hand.

Furthermore, the validity of the present CB tracing methodology deserves further debate. The diffusion and the uptake of the CB tracer under the skin at the injection sites in each finger/toe phalange may be variable across fingers and monkeys. As far as inter-individual variability is concerned, an important player may be the unavoidable variation across CB immune-reactions performed at different time points and different series of histological sections, in addition to the possible impact on the quality of tissue fixation and preservation. However, the inter-individual variability did not strongly impact the present data as the extent (area) of CB labeling was not systematically compared across monkeys. The quantitative statistical analysis was focused on an intra-individual comparison of one side of the gracile or cuneate nucleus with its counterpart on the other side. Such bilateral comparison within a single animal is therefore minimally impacted by differences in tissue fixation and/or processing. In other words, the analysis was aimed to assess whether the experimental manipulations (lesion, treatment) impacted on a balance or imbalance of bilateral CB labeling area.

Keeping in mind the obvious limitation resulting from the small number of subjects per group, the present study pointed out interesting information regarding the preservation of the DCN organization following motor system injury. Concerning inter-finger/toe variability, limited to some extent by injecting the same volumes of CB on each side, the gracile and cuneate nuclei CB data in the intact monkeys ( $n=2$ ) are consistent with the notion that no statistically significant bilateral difference

should be present. In these 2 intact monkeys, the absence of bilateral difference was observed for both DCN nuclei, making overall 4 coherent observations suggesting that the inter-finger/toe variability did not play a major role. Furthermore, going in the same direction, 1 SCI monkey subjected to a control (not effective) antibody treatment exhibited the expected bilateral imbalance, with a lower extent of the CB labeling on the ipsilesional side of the gracile nucleus (Mk-C-Bo; Figure 3C). Moreover, the same control animal with SCI showed an absence of impact of the SCI at C7-C8 level on the bilateral extent of CB labeling in the cuneate nucleus (Figure 4C). Taken together, these 6 observations provide some evidence that the intra-individual bilateral comparison of CB labeling extent appears reliable, so that possible effects of the treatments tested here on the primary somatosensory inputs from the first 2 fingers/toes can be tentatively assessed.

As far as SCI is concerned, the data of Figure 3 show that the mixed treatment anti-Nogo-A antibody/BDNF did not counterbalance the bilateral asymmetry, with a lower extent of the primary inputs in the ipsilesional gracile nucleus. On the contrary, compared with the control antibody-treated monkey (Figure 3C), the 2 monkeys subjected to the mixed treatment exhibited an even more pronounced bilateral imbalance (Figure 3D). After SCI, but in the cuneate nuclei, the CB labeling area did not show a bilateral imbalance in 2 out of 3 animals subjected to the mixed treatment (Figure 4D), similar to what was observed in absence of treatment (control antibody, Figure 4C). The exception is monkey Mk-AB-P exhibiting a statistically significant bilateral difference (Figure 4D). Nevertheless, the significance is moderate ( $P = .03$ ) as some sections also showed the reverse tendency (lesioned side, the black bars, higher than the unlesioned side, the gray ones). These data also show that the mixed treatment did not impact on the cuneate nucleus primary inputs after SCI, in line with what was observed for the gracile nucleus. Overall, the lack of an apparent effect of the combined anti-Nogo-A/BDNF treatment on the bilateral distribution of cutaneous inputs in the dorsal column nuclei (Figures 3 and 4) is coherent with the observation that such combined treatment only had a moderate impact in promoting the functional recovery after SCI, clearly lower than the significant enhancement of functional recovery obtained when anti-Nogo-A antibody was applied alone.<sup>40</sup>

Finally, the monkeys subjected to MCI without treatment (Figure 5C) did not show any significant bilateral difference of CB labeling area in the cuneate nucleus, and the present data do not support the possibility of a remote effect due to connectional diaschisis at distance. Interestingly, a significant bilateral difference was observed in the 2 MCI monkeys treated with the anti-Nogo-A antibody alone (Figure 5D) whereas the MCI monkeys not receiving the treatment did not show a significant bilateral difference. However the bilateral bias is in the same direction in the 2 monkeys, the labeled area of the lesioned side (in black) being larger than on the unlesioned side (in gray), the level of significance is moderate especially for 1 of

these 2 monkeys (Mk-A-SI,  $P = .04$  and Mk-A-Mo,  $P = .003$ ; Figure 5). These data may suggest an effect of the anti-Nogo-A antibody treatment on primary inputs in the cuneate nucleus after MCI as it links the more remote effects observed by Thallmair et al.<sup>22</sup> They have observed regeneration of lesioned pyramidal projections to the sensory dorsal column nuclei (DCN) in the brainstem after pyramidotomy in the rodent. However, as a consequence of the weak statistical significance and the limited number of subjects, there is no strong evidence here in favor of an effect of the anti-Nogo-A antibody treatment on primary inputs in the cuneate nucleus after MCI. These data highlight the need to assess the possible role of more remote effects of the anti-Nogo-A antibody treatment. Overall, in both SCI and MCI models, the investigated 2 treatments did not influence strongly the primary sensory (cutaneous) inputs to DCN. The effects of these treatments on the functional recovery of manual dexterity from the SCI and from MCI have been reported previously.<sup>30,40</sup> In monkeys subjected to MCI or SCI, a treatment with anti-Nogo-A antibody exhibited a significant improvement of the functional recovery as compared to monkeys in the control groups. In case of SCI, as the anti-Nogo-A antibody treatment itself led to complete functional recovery following the SCI performed at C7-C8 level by Freund et al,<sup>19,27</sup> to test a potential beneficial effect of BDNF added to anti-Nogo-A antibody, it was necessary to perform clearly larger SCI lesions at C7-C8 level, inducing more severe deficits.<sup>40</sup> It turned out that BDNF combined with anti-Nogo-A antibody did not functionally compensate for the extra deleterious effect caused by the larger SCI, although the functional recovery in monkeys subjected to the combined treatment still remained significantly better than in monkeys which received a control antibody only.<sup>40</sup> However, the small number of monkeys involved in the present CB tracing does not allow a precise correlation of the tracing data with the behavioral data reflecting the level of functional recovery in individual monkeys. Even in absence of effects on the connectivity as observed here with CB tracing, an electrophysiological study would still be able to reveal functional consequences at distance (diaschisis) due to remote motor system injuries in the somatosensory pathways at the brainstem level.

#### *Links with previous reports*

To our knowledge, the present study is the first one to report on the transganglionic tracing of primary somatosensory afferents from the hand and the foot in case of SCI at the cervical level (hemi-section) or MCI. Post-lesional transganglionic tracing of primary afferents in the cuneate nucleus has been reported,<sup>61</sup> but for a very different type of injury, namely a rhizotomy (dorsal rootlet section) restricted to C8 level. Furthermore, the present study extends the data for the hand (cuneate nucleus) to the foot (gracile nucleus). Finally, we have conducted the first approach in order to assess the possible impact of regenerative treatments on the primary afferent projections to DCN after SCI or MCI.



As far as the topographical distribution of CB-labeling in the cuneate/gracile nuclei is concerned, corresponding to primary somatosensory inputs from the first 2 fingers/toes, the present data (Figures 3–5) are consistent with previous reports in non-human primates.<sup>61,63,65–67</sup> In the cuneate nucleus, the primary afferents from digits D1 and D2 are ventrally located and form a rostrocaudally located elongated column, as reported by Florence et al.<sup>62,63</sup> This topography in the cuneate nucleus in macaques was found to be somewhat different from that observed in the squirrel monkey.<sup>64,70</sup> In the gracile nucleus, cutaneous afferents from the first 2 toes formed patchy labeling territories, along with the rostrocaudal extent of the nucleus, as previously reported.<sup>66,67</sup>

As a result of transection of the posterior column in monkeys (a lesional territory included in the present SCI monkeys), it was reported that the neuronal population in the gracile nucleus did not change. However, there were transneuronal changes affecting the denervated neurons, showing a decrease in the cell body area and nuclear area.<sup>71</sup> Such transneuronal changes of gracile neurons were not the topic of the present study, limited to the bilateral effect on the primary afferents from the hand and foot.

As a result of a restricted unilateral rhizotomy at C8 level, by comparing 2 time points post-lesion, it was demonstrated that the large number of primary afferents spared by the lesion on the ipsilesional side gave rise to compensatory sprouting of their axonal terminals in the cuneate nucleus.<sup>61</sup> The question then arises regarding the possibility that such sprouting takes place in the present model of SCI. As shown in Figure 2, the 4 monkeys subjected to SCI exhibit a nearly complete transection of the dorsal funiculi. As a result, the number of ascending axons preserved by the transection on the lesioned side is small, suggesting that compensatory sprouting was most likely limited and thus may have little impacted on the bilateral balance of CB labeled terminals areas in the gracile and cuneate nuclei. With a nearly complete hemi-section, including most of the dorsal funiculi, the limited sprouting on the ipsilesional side may leave open the possibility of compensatory sprouting from the intact contralateral primary afferents, although it is unknown whether some afferents can cross the midline and, if yes, to what extent.

## Acknowledgements

Thanks are due to Dr Thierry Wannier for his valuable contribution to early phases of the study, as well as to Prof ME Schwab and Dr A Mir for their contribution to the design of the anti-Nogo-A antibody treatment. The authors thank the excellent technical assistance of Mrs Véronique Moret, Christine Roulin, and Christiane Marti (histology), of Mr Laurent Bossy, Joseph Corpataux, and Jacques Maillard (animal care taking), André Gaillard (mechanics), Bernard Aebischer (electronics), and Laurent Monney (informatics). We thank Dr S Bashir, and A Wyss for participation in some behavioral experiments.

## Authors' Contribution

JS performed most of the analysis of the histological data; MLB and EMR performed the in vivo experiments and tracer injections; JS and EMR prepared the figures; JS and EMR wrote the manuscript for the most part, all authors edited the text; JS and EMR designed and supervised the morphological analysis; EMR and MLB designed and coordinated the overall behavioral and lesional study.

## ORCID iD

Julie Savidan  <https://orcid.org/0000-0002-9305-2808>

## REFERENCES

1. Dancause N. Vicarious function of remote cortex following stroke: recent evidence from human and animal studies. *Neuroscientist*. 2006;12:489–499.
2. Nudo RJ, Friel KM, Delia SW. Role of sensory deficits in motor impairments after injury to primary motor cortex. *Neuropharmacology*. 2000;39:733–742. doi:10.1016/s0028-3908(99)00254-3
3. Nudo RJ. Mechanisms for recovery of motor function following cortical damage. *Curr Opin Neurobiol*. 2006;16:638–644. doi:10.1016/j.conb.2006.10.004
4. Von Monakow C. *Die Lokalisation Im Grosshirn Und Der Abbau Der Funktion Durch Kortikale Herde*. JF Bergmann; 1914.
5. Carrera E, Tononi G. Diaschisis: past, present, future. *Brain*. 2014;137:2408–2422.
6. Cheema S, Rustioni A, Whitsel BL. Sensorimotor cortical projections to the primate cuneate nucleus. *J Comp Neurol*. 1985;240:196–211.
7. Chambers WW, Liu C-N. Cortico-spinal tract of the cat. An attempt to correlate the pattern of degeneration with deficits in reflex activity following neocortical lesions. *J Comp Neurol*. 1957;108:23–55.
8. Martinez L, Lamas JA, Canedo A. Pyramidal tract and corticospinal neurons with branching axons to the dorsal column nuclei of the cat. *Neuroscience*. 1995;68:195–206. doi:10.1016/0306-4522(95)00133-4
9. Bentivoglio M, Rustioni A. Corticospinal neurons with branching axons to the dorsal column nuclei in the monkey. *J Comp Neurol*. 1986;253:260–276.
10. Kuypers HG, Tuerk JD. The distribution of the cortical fibres within the nuclei cuneatus and gracilis in the cat. *J Anat*. 1964;98:143–162.
11. Caroni P, Schwab ME. Antibody against myelin-associated inhibitor of neurite growth neutralizes nonpermissive substrate properties of CNS white matter. *Neuron*. 1988;1:85–96. doi:10.1016/0896-6273(88)90212-7
12. GrandPré T, Nakamura F, Vartanian T, Strittmatter SM. Identification of the Nogo inhibitor of axon regeneration as a Reticulon protein. *Nature*. 2000;403:439–444. doi:10.1038/35000226
13. Buchli AD, Schwab ME. Inhibition of Nogo: a key strategy to increase regeneration, plasticity and functional recovery of the lesioned central nervous system. *Ann Med*. 2005;37:556–567.
14. Zörner B, Schwab ME. Anti-Nogo on the go: from animal models to a clinical trial. *Ann NY Acad Sci*. 2010;1198:E22–E34. doi:10.1111/j.1749-6632.2010.05566.x
15. Wang T, Xiong J-Q, Ren X-B, Sun W. The role of Nogo-A in neuroregeneration: a review. *Brain Res Bull*. 2012;87:499–503. doi:10.1016/j.brainresbull.2012.02.011
16. Schwab ME. Nogo and axon regeneration. *Curr Opin Neurobiol*. 2004;14:118–124. doi:10.1016/j.conb.2004.01.004
17. Pernet V, Schwab ME. The role of Nogo-A in axonal plasticity, regrowth and repair. *Cell Tissue Res*. 2012;349:97–104. doi:10.1007/s00441-012-1432-6
18. Schwab ME, Strittmatter SM. Nogo limits neuronal plasticity and recovery from injury. *Curr Opin Neurobiol*. 2014;27:53–60. doi:10.1016/j.conb.2014.02.011
19. Freund P, Schmidlin E, Wannier T, et al. Anti-Nogo-A antibody treatment promotes recovery of manual dexterity after unilateral cervical lesion in adult primates—re-examination and extension of behavioral data. *Eur J Neurosci*. 2009;29:983–996. doi:10.1111/j.1460-9568.2009.06642.x
20. Harvey PA, Lee DHS, Qian F, Weinreb PH, Frank E. Blockade of Nogo receptor ligands promotes functional regeneration of sensory axons after dorsal root crush. *J Neurosci Off J Soc Neurosci*. 2009;29:6285–6295. doi:10.1523/JNEUROSCI.5885-08.2009
21. Schnell L, Schwab ME. Sprouting and regeneration of lesioned corticospinal tract fibres in the adult rat spinal cord. *Eur J Neurosci*. 1993;5:1156–1171. doi:10.1111/j.1460-9568.1993.tb00970.x
22. Thallmair M, Metz GA, Z'Graggen WJ, Raineteau O, Kartje GL, Schwab ME. Neurite growth inhibitors restrict plasticity and functional recovery following corticospinal tract lesions. *Nat Neurosci*. 1998;1:124–131. doi:10.1038/373



23. Papadopoulos CM, Tsai S-Y, Alsbici T, O'Brien TE, Schwab ME, Kartje GL. Functional recovery and neuroanatomical plasticity following middle cerebral artery occlusion and IN-1 antibody treatment in the adult rat. *Ann Neurol*. 2002;51:433-441. doi:10.1002/ana.10144
24. Li S, Strittmatter SM. Delayed systemic Nogo-66 receptor antagonist promotes recovery from spinal cord injury. *J Neurosci Off J Soc Neurosci*. 2003;23:4219-4227.
25. Lee J-K, Kim J-E, Sivula M, Strittmatter SM. Nogo receptor antagonism promotes stroke recovery by enhancing axonal plasticity. *J Neurosci Off J Soc Neurosci*. 2004;24:6209-6217. doi:10.1523/JNEUROSCI.1643-04.2004
26. Fouad K, Klusman I, Schwab ME. Regenerating corticospinal fibers in the Marmoset (*Callitrix jacchus*) after spinal cord lesion and treatment with the anti-Nogo-A antibody IN-1. *Eur J Neurosci*. 2004;20:2479-2482. doi:10.1111/j.1460-9568.2004.03716.x
27. Freund P, Schmidlin E, Wannier T, et al. Nogo-A-specific antibody treatment enhances sprouting and functional recovery after cervical lesion in adult primates. *Nat Med*. 2006;12:790-792. doi:10.1038/nm1436
28. Freund P, Wannier T, Schmidlin E, et al. Anti-Nogo-A antibody treatment enhances sprouting of corticospinal axons rostral to a unilateral cervical spinal cord lesion in adult macaque monkey. *J Comp Neurol*. 2007;502:644-659. doi:10.1002/cne.21321
29. Hamadjida A, Wyss AF, Mir A, Schwab ME, Belhaj-Saif A, Rouiller EM. Influence of anti-Nogo-A antibody treatment on the reorganization of callosal connectivity of the premotor cortical areas following unilateral lesion of primary motor cortex (M1) in adult macaque monkeys. *Exp Brain Res*. 2012;223:321-340.
30. Wyss AF, Hamadjida A, Savidan J, et al. Long-term motor cortical map changes following unilateral lesion of the hand representation in the motor cortex in macaque monkeys showing functional recovery of hand functions. *Restor Neurol Neurosci*. 2013;31:733-760. doi:10.3233/RNN-130344
31. Hoogewoud F, Hamadjida A, Wyss AF, et al. Comparison of functional recovery of manual dexterity after unilateral spinal cord lesion or motor cortex lesion in adult macaque monkeys. *Front Neurol*. 2013;4:101. doi:10.3389/fneur.2013.00101
32. Fregosi M, Contestabile A, Badoud S, et al. Changes of motor corticobulbar projections following different lesion types affecting the central nervous system in adult macaque monkeys. *Eur J Neurosci*. 2018;48:2050-2070. doi:10.1111/ejn.14074
33. Kucher K, Johns D, Maier D, et al. First-in-man intrathecal application of neurite growth-promoting anti-Nogo-A antibodies in acute spinal cord injury. *Neurorehabil Neural Repair*. 2018;32:578-589. doi:10.1177/1545968318776371
34. Barde Y-A, Edgar D, Thoenen H. Purification of a new neurotrophic factor from mammalian brain. *EMBO J*. 1982;1:549-553.
35. Sasaki M, Radtke C, Tan AM, et al. BDNF-hypersecreting human mesenchymal stem cells promote functional recovery, axonal sprouting, and protection of corticospinal neurons after spinal cord injury. *J Neurosci Off J Soc Neurosci*. 2009;29:14932-14941. doi:10.1523/JNEUROSCI.2769-09.2009
36. Weishaupt N, Blesch A, Fouad K. BDNF: the career of a multifaceted neurotrophin in spinal cord injury. *Exp Neurol*. 2012;238:254-264. doi:10.1016/j.expneurol.2012.09.001
37. Jin Y, Fischer I, Tessler A, Houle JD. Transplants of fibroblasts genetically modified to express BDNF promote axonal regeneration from supraspinal neurons following chronic spinal cord injury. *Exp Neurol*. 2002;177:265-275. doi:10.1006/exnr.2002.7980
38. Menei P, Montero-Menei C, Whittemore SR, Bunge RP, Bunge MB. Schwann cells genetically modified to secrete human BDNF promote enhanced axonal regrowth across transected adult rat spinal cord. *Eur J Neurosci*. 1998;10:607-621. doi:10.1046/j.1460-9568.1998.00071.x
39. Lu P, Tuszynski MH. Growth factors and combinatorial therapies for CNS regeneration. *Exp Neurol*. 2008;209:313-320. doi:10.1016/j.expneurol.2007.08.004
40. Beaud M-L, Rouiller EM, Bloch J, Mir A, Schwab ME, Schmidlin E. Combined with anti-Nogo-A antibody treatment, BDNF did not compensate the extra deleterious motor effect caused by large size cervical cord hemisection in adult macaques. *CNS Neurosci Ther*. 2020;26:260-269. doi:10.1111/cns.13213
41. Song X-Y, Li F, Zhang F-H, Zhong J-H, Zhou X-F. Peripherally-derived BDNF promotes regeneration of ascending sensory neurons after spinal cord injury. *PLoS ONE*. 2008;3:e1707. doi:10.1371/journal.pone.0001707
42. Bregman BS, McAtee M, Dai HN, Kuhn PL. Neurotrophic factors increase axonal growth after spinal cord injury and transplantation in the adult rat. *Exp Neurol*. 1997;148:475-494.
43. Oudega M, Hagg T. Neurotrophins promote regeneration of sensory axons in the adult rat spinal cord. *Brain Res*. 1999;818:431-438. doi:10.1016/S0006-8993(98)01314-6
44. Vavrek R, Girgis J, Tetzlaff W, Hiebert GW, Fouad K. BDNF promotes connections of corticospinal neurons onto spared descending interneurons in spinal cord injured rats. *Brain J Neurol*. 2006;129:1534-1545. doi:10.1093/brain/awl087
45. Hollis ER, Jamshidi P, Löw K, Blesch A, Tuszynski MH. Induction of corticospinal regeneration by lentiviral trkB-induced Erk activation. *Proc Natl Acad Sci USA*. 2009;106:7215-7220. doi:10.1073/pnas.0810624106
46. Darian-Smith C. Monkey models of recovery of voluntary hand movement after spinal cord and dorsal root injury. *ILAR J*. 2007;48:396-410.
47. Beaud M-L, Schmidlin E, Wannier T, et al. Anti-Nogo-A antibody treatment does not prevent cell body shrinkage in the motor cortex in adult monkeys subjected to unilateral cervical cord lesion. *BMC Neurosci*. 2008;9:5.
48. Beaud M-L, Rouiller EM, Bloch J, et al. Invasion of lesion territory by regenerating fibers after spinal cord injury in adult macaque monkeys. *Neuroscience*. 2012;227:271-282.
49. Wannier-Morino P, Schmidlin E, Freund P, et al. Fate of rubrospinal neurons after unilateral section of the cervical spinal cord in adult macaque monkeys: effects of an antibody treatment neutralizing Nogo-A. *Brain Res*. 2008;1217:96-109. doi:10.1016/j.brainres.2007.11.019
50. Kaeser M, Wyss AF, Bashir S, et al. Effects of unilateral motor cortex lesion on ipsilesional hand's reach and grasp performance in monkeys: relationship with recovery in the contralesional hand. *J Neurophysiol*. 2010;103:1630-1645. doi:10.1152/jn.00459.2009
51. Bashir S, Kaeser M, Wyss A, et al. Short-term effects of unilateral lesion of the primary motor cortex (M1) on ipsilesional hand dexterity in adult macaque monkeys. *Brain Struct Funct*. 2012;217:63-79.
52. Schmidlin E, Wannier T, Bloch J, Rouiller EM. Progressive plastic changes in the hand representation of the primary motor cortex parallel incomplete recovery from a unilateral section of the corticospinal tract at cervical level in monkeys. *Brain Res*. 2004;1017:172-183. doi:10.1016/j.brainres.2004.05.036
53. Schmidlin E, Wannier T, Bloch J, Belhaj-Saif A, Wyss AF, Rouiller EM. Reduction of the hand representation in the ipsilateral primary motor cortex following unilateral section of the corticospinal tract at cervical level in monkeys. *BMC Neurosci*. 2005;6:56. doi:10.1186/1471-2202-6-56
54. Schmidlin E, Kaeser M, Gindrat A-D, et al. Behavioral assessment of manual dexterity in non-human primates. *J Vis Exp*. 2011;57:3258. doi:10.3791/3258
55. Wannier T, Schmidlin E, Bloch J, Rouiller EM. A unilateral section of the corticospinal tract at cervical level in primate does not lead to measurable cell loss in motor cortex. *J Neurotrauma*. 2005;22:703-717. doi:10.1089/neu.2005.22.703
56. Jenny AB, Inukai J. Principles of motor organization of the monkey cervical spinal cord. *J Neurosci*. 1983;3:567-575.
57. Liu Y, Rouiller EM. Mechanisms of recovery of dexterity following unilateral lesion of the sensorimotor cortex in adult monkeys. *Exp Brain Res*. 1999;128:149-159. doi:10.1007/s002210050830
58. Savidan J, Kaeser M, Belhaj-Saif A, Schmidlin E, Rouiller EM. Role of primary motor cortex in the control of manual dexterity assessed via sequential bilateral lesion in the adult macaque monkey: a case study. *Neuroscience*. 2017;357:303-324. doi:10.1016/j.neuroscience.2017.06.018
59. Oertle T, van der Haar ME, Bandtlow CE, et al. Nogo-A inhibits neurite outgrowth and cell spreading with three discrete regions. *J Neurosci Off J Soc Neurosci*. 2003;23:5393-5406.
60. Weinmann O, Schnell L, Ghosh A, et al. Intrathecally infused antibodies against Nogo-A penetrate the CNS and downregulate the endogenous neurite growth inhibitor Nogo-A. *Mol Cell Neurosci*. 2006;32:161-173. doi:10.1016/j.mcn.2006.03.007
61. Darian-Smith C. Primary afferent terminal sprouting after a cervical dorsal rootlet section in the macaque monkey. *J Comp Neurol*. 2004;470:134-150.
62. Florence SL, Wall JT, Kaas JH. The somatotopic pattern of afferent projections from the digits to the spinal cord and cuneate nucleus in macaque monkeys. *Brain Res*. 1988;452:388-392.
63. Florence SL, Wall JT, Kaas JH. Somatotopic organization of inputs from the hand to the spinal gray and cuneate nucleus of monkeys with observations on the cuneate nucleus of humans. *J Comp Neurol*. 1989;286:48-70.
64. Florence SL, Wall JT, Kaas JH. Central projections from the skin of the hand in squirrel monkeys. *J Comp Neurol*. 1991;311:563-578. doi:10.1002/cne.903110410
65. Culbertson JL, Brushart TM. Somatotopy of digital nerve projections to the cuneate nucleus in the monkey. *Somatosens Mot Res*. 1989;6:319-330.
66. Strata F, Coq J-O, Kaas JH. The chemo- and somatotopic architecture of the Galago cuneate and gracile nuclei. *Neuroscience*. 2003;116:831-850. doi:10.1016/S0306-4522(02)00694-2
67. Qi H-X, Kaas JH. Organization of primary afferent projections to the gracile nucleus of the dorsal column system of primates. *J Comp Neurol*. 2006;499:183-217. doi:10.1002/cne.21061
68. Pizzimenti MA, Darling WG, Rotella DL, et al. Measurement of reaching kinematics and prehensile dexterity in nonhuman primates. *J Neurophysiol*. 2007;98:1015-1029. doi:10.1152/jn.00354.2007
69. Rouiller EM, Babalian A, Kazennikov O, Moret V, Yu XH, Wiesendanger M. Transcallosal connections of the distal forelimb representations of the primary and supplementary motor cortical areas in macaque monkeys. *Exp Brain Res*. 1994;102:227-243. doi:10.1007/bf00227511
70. Xu J, Wall JT. Functional organization of tactile inputs from the hand in the cuneate nucleus and its relationship to organization in the somatosensory cortex. *J Comp Neurol*. 1999;411:369-389.
71. Loewy AD. Transneuronal changes in the gracile nucleus. *J Comp Neurol*. 1973;147:497-510. doi:10.1002/cne.901470405